Journal of Thermodynamics & Catalysis
ISSN: 2157-7544

Trivedi et al., J Thermodyn Catal 2015, 6:3
DOI: 10.4172/2157-7544.1000151

Research article Open Access

Biofield Energy Treatment: A Potential Strategy for Modulating Physical, Thermal and Spectral Properties of 3-Chloro-4-fluoroaniline

Mahendra Kumar Trivedi[1], Rama Mohan Tallapragada[1], Alice Branton[1], Dahryn Trivedi[1], Gopal Nayak[1], Rakesh Kumar Mishra[2] and Snehasis Jana[2*]

[1]*Trivedi Global Inc., 10624 S Eastern Avenue Suite A-969, Henderson, NV 89052, USA*
[2]*Trivedi Science Research Laboratory Pvt. Ltd., Hall-A, Chinar Mega Mall, Chinar Fortune City, Hoshangabad Rd., Bhopal, Madhya Pradesh, India*

Abstract

3-Chloro-4-fluoroaniline (CFA) is used as an intermediate for the synthesis of pharmaceutical compounds. The objective of this study was to investigate the influence of biofield energy treatment on the physical, thermal and spectral properties of CFA. The study was performed in two groups (control and treated). The control group remained as untreated, and the treated group received Mr. Trivedi's biofield energy treatment. The control and treated CFA samples were further characterized by x-ray diffraction (XRD), differential scanning calorimetry (DSC), thermogravimetric analysis (TGA), fourier transform infrared (FT-IR) spectroscopy, and ultra violet-visible spectroscopy (UV-vis) analysis. The XRD analysis of treated CFA showed significant changes in the intensity of peaks as compared to the control. However, the average crystallite size (G) was significantly decreased by 22.08% in the treated CFA with respect to the control. The DSC analysis showed slight decrease in the melting temperature of treated CFA (47.56°C) as compared to the control (48.05°C). However, the latent heat of fusion in the treated sample was considerably changed by 4.28% with respect to the control. TGA analysis showed increase in maximum thermal decomposition temperature (Tmax) of the treated sample (163.34°C) as compared to the control sample (159.97°C). Moreover the onset temperature of treated CFA (148 °C) was also increased as compared to the control sample (140°C). Additionally, the weight loss of the treated sample was reduced (42.22%) with respect to the control (56.04%) that may be associated with increase in thermal stability. The FT-IR spectroscopic evaluation showed emergence of one new peak at 3639 cm-1 and alteration of the N-H (stretching and bending) peak in the treated sample as compared to the control. Overall, the result demonstrated that Mr. Trivedi's biofield energy treatment has paramount influence on the physical, thermal and spectral properties of CFA.

Keywords: 3-Chloro-4-Fluoroaniline; Biofield energy treatment; Thermal analysis; X-ray diffraction; Fourier transform infrared analysis; Ultra violet-visible spectroscopy

Abbreviations: CFA: 3-Chloro-4-fluoroaniline; XRD: X-Ray Diffraction; DSC: Differential Scanning Calorimetry; TGA: Thermo Gravimetric Analysis; FT-IR: Fourier Transform Infrared Spectroscopy; UV-vis: Ultra Violet-Visible Spectroscopy; CAM: Complementary and Alternative Medicine

Introduction

The amine derivatives are used as the building units in the construction of channel type supramolecular structure revealing its catalytic and separation properties due to their ability to generate intermolecular interactions [1,2]. 3-Chloro-4-fluoroaniline (CFA) is an amine derivative which is used as intermediate compound for the synthesis of herbicides [3]. Moreover, CFA is used as an intermediate for the synthesis of ciprofloxacin hydrochloride which is approved for the treatment of bone, joint infections, diarrhea, lower respiratory tract infections, and urinary tract infections [4]. Further, CFA is also used for the synthesis of norfloxacin that is the first representative of fluorinated quinolone derivatives. Norfloxacin drug has wide antimicrobial actions, and it was approved for the treatment of respiratory tract, ear, throat, nose and other infective and inflammatory diseases [5]. The chemical and physical stability of the pharmaceutical compounds are more desired quality attributes that directly affect its safety, efficacy, and shelf life [6]. Hence, it is required to explore some new alternate approach that could alter the physical and thermal properties of the compounds. Recently, biofield energy treatment has substantially changed the physical and thermal properties of metals [7,8], ceramics [9], organic product [10] and spectral properties of various pharmaceutical drugs [11]. After considering the pharmaceutical applications of CFA as intermediate, authors wish to investigate the impact of biofield energy treatment on CFA and analyzed its physical, thermal and spectral properties. The National Center for Complementary and Alternative Medicine (NCCAM), a part of the National Institute of Health (NIH), recommends the use of Complementary and Alternative Medicine (CAM) therapies as an alternative to the healthcare sector and about 36% of Americans regularly uses some form of CAM [12]. CAM includes numerous energy-healing therapies; biofield therapy is one of the energy medicine used worldwide to improve the health. The biofield treatment is being used in healing process to reduce pain, anxiety and to promote the overall health of human being [13,14]. Recently it was discovered that electrical process occurring in the human body has a relation with the magnetic field. According to Ampere's law, the moving charge produces the magnetic field in surrounding space. Likewise, human body emits the electromagnetic waves in the form of bio-photons, which surrounds the body, and it is commonly known as biofield. Therefore, the biofield consists of an electromagnetic field, being generated by moving electrically charged particles (ions,

***Corresponding author:** Snehasis Jana, Trivedi Science Research Laboratory Pvt. Ltd., Hall-A, Chinar Mega Mall, Chinar Fortune City, Hoshangabad Rd., Bhopal-462 026, Madhya Pradesh, India, Tel: 917556660006; E-mail: publication@trivedisrl.com

Received September 01, 2015; **Accepted** October 01, 2015; **Published** October 15, 2015

Citation: Trivedi MK, Tallapragada RM, Branton A, Trivedi D, Nayak G, et al. (2015) Biofield Energy Treatment: A Potential Strategy for Modulating Physical, Thermal and Spectral Properties of 3-Chloro-4-fluoroaniline. J Thermodyn Catal 6: 151. doi:10.4172/2157-7544.1000151

cell, molecule, etc.) inside the human body [15,16]. Rivera-Ruiz *et al.* reported that electrocardiography has been extensively used to measure the biofield energy of the human body [17]. Thus, human beings have the ability to harness the energy from the environment/Universe and can transmit into any object (living or non-living) around the Globe. The object(s) will always receive the energy and responding in a useful manner that is called biofield energy. Mr. Trivedi's unique biofield treatment is also known as The Trivedi Effect®. Mr. It is known to transform the characteristics of various living and nonliving things. Moreover, the biofield treatment has improved the growth and production of agriculture crops [18-20] and significantly altered the phenotypic characteristics of various pathogenic microbes [21,22]. The present work was focused to study the impact of biofield treatment on physical, thermal and spectral properties of CFA and characterized by XRD, DSC, TGA, FT-IR and UV-visible spectroscopy analysis.

Materials and Methods

3-Chloro-4-fluoroaniline (CFA) was procured from Sisco Research Laboratories (SRL), India.

Biofield treatment

CFA was divided into two parts; one was kept as a control sample, while the other was subjected to Mr. Trivedi's biofield treatment and coded as treated sample. The treatment group was in sealed pack and handed over to Mr. Trivedi for biofield treatment under laboratory condition. Mr. Trivedi provided the treatment through his energy transmission process to the treated group without touching the sample. After biofield treatment the control and treated group was subjected to physicochemical characterization under standard laboratory conditions. The control and treated samples were characterized by XRD, DSC, TGA, FT-IR, and UV-visible analysis.

Characterization

X-ray diffraction (XRD) study: XRD analysis of control and treated CFA was carried out on Phillips, Holland PW 1710 X-ray diffractometer system, which had a copper anode with nickel filter. The radiation of wavelength used by the XRD system was 1.54056 Å. The data obtained from this XRD were in the form of a chart of 2θ *vs.* intensity and a detailed table containing peak intensity counts, d value (Å), peak width (θ°), relative intensity (%) etc. The average crystallite size (G) was calculated by using formula:

$$G=k\lambda/(b\cos\theta)$$

Here, λ is the wavelength of radiation used, b is full width half-maximum (FWHM) of peaks and k is the equipment constant (=0.94).

Percentage change in average crystallite size was calculated using following formula:

$$\text{Percentage change in crystallite size}=[(G_t-G_c)/G_c]\times 100$$

Where, G_c and G_t are the crystallite size of control and treated powder samples respectively.

Differential scanning calorimetry (DSC)

DSC was used to investigate the melting temperature and latent heat of fusion (ΔH) of samples. The control and treated CFA samples were analyzed using a Pyris-6 Perkin Elmer DSC at a heating rate of 10°C/min under air atmosphere and the air was flushed at a flow rate of 5 mL/min. Predetermined amount of sample was kept in an aluminum pan and closed with a lid. A blank aluminum pan was used as a reference. The percentage change in latent heat of fusion was calculated using following equations:

$$\%\,\text{Change in latent heat of fusion}=\frac{[\Delta H_{\text{Treated}}-\Delta H_{\text{Control}}]}{\Delta H_{\text{Control}}}\times 100$$

Where, $\Delta H_{\text{Control}}$ and $\Delta H_{\text{Treated}}$ are the latent heat of fusion of control and treated samples, respectively.

Thermogravimetric analysis-differential thermal analysis (TGA-DTA)

The thermal stability of control and treated CFA were analyzed by using Mettler Toledo simultaneous TGA and Differential thermal analyzer (DTA). The samples were heated from room temperature to 400°C with a heating rate of 5°C/min under air atmosphere.

FT-IR spectroscopy

The FT-IR spectra were recorded on Shimadzu's Fourier transform infrared spectrometer (Japan) with the frequency range of 4000-500 cm^{-1}. The analysis was accomplished to evaluate the effect of biofield treatment at an atomic level like dipole moment, force constant and bond strength in chemical structure [23]. The treated sample was divided in two parts T1 and T2 for FT-IR analysis.

UV-Vis spectroscopic analysis

UV spectra of the control and treated CFA samples were recorded on Shimadzu UV-2400 PC series spectrophotometer with 1 cm quartz cell and a slit width of 2.0 nm. The spectroscopic analysis was carried out using wavelength in the range of 200-400 nm and methanol was used as a solvent. The UV spectra was analyzed to determine the effect of biofield treatment on the energy gap of highest occupied molecular orbital and lowest unoccupied molecular orbital (HOMO–LUMO gap) [23]. The treated sample was divided in two parts T1 and T2 for the UV-Vis spectroscopic analysis.

Results and Discussion

XRD analysis

The XRD diffractogram of control and treated CFA are shown in Figure 1. XRD diffractogram of the control CFA sample showed intense crystalline peaks that can be correlated to its crystalline nature. The XRD diffractogram showed peaks at 2θ equal to 13.10°, 20.58°, 22.16°, 22.29°, and 28.40°. However, the treated sample also showed intense crystalline peaks at 2θ equal to 20.73°, 22.12°, 23.08°, 29.97°, and 30.30°. The XRD peaks originally present at 2-theta equal to 20.58°, 28.40°, 29.77° and 30.33° were shifted to Bragg's angle 2-theta equal to 20.73°, 28.37°, 29.97° and 30.30°. The intensities of these XRD peaks were increased substantially as compared to the control. This may be inferred as increase in the crystallinity of the treated CFA as compared to the control. The crystallite size was calculated using Scherrer formula and the results are presented in Figure 2. The crystallite size of the control sample was 94.80 nm, and it was decreased to 73.86 nm in the treated sample. The crystallite size was decreased by 22.08% in treated CFA with respect to control. The decrease in crystallite size of treated sample could be ascribed to biofield treatment that may cause increase in compressive stress that leads to increase in dislocation density and decrease in crystallite size. Zhao *et al.* showed that increase in compressive stress in the material causes decrease in crystallite size [24]. Moreover, Schicker *et al.* reported that crystallite size is inversely proportional to the milling speed, thus increase in milling speed decreases the crystallite size [25,26]. Mahmoud *et al.* reported that

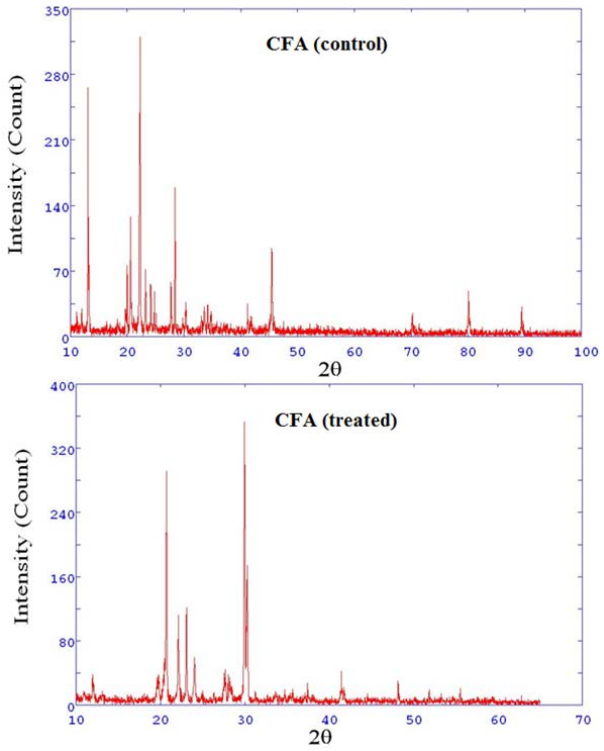

Figure 1: XRD diffractogram of control and treated 3-chloro-4-fluoroaniline.

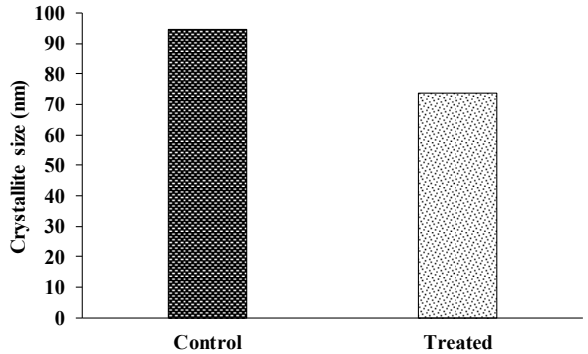

Figure 2: Crystallite size of control and treated 3-chloro-4-fluoroaniline.

lattice strain induced by mechanical milling may causes a significant reduction in crystallite size [27]. Previously our research group reported that biofield treatment had substantially reduced the crystallite size of vanadium pentoxide powders. It was proposed that internal strains made dislocations to move on the slip planes and intersecting slip planes built in stress concentration to such an extent causing the crystal to fracture at the sub boundaries [9]. Hence, it is assumed here that biofield energy treatment may provide the compressive stress through energy milling, which may lead to the reduction in the crystallite size of treated CFA as compared to the control.

It was previously suggested that nano scale particle size and small crystallite size can overcome slow diffusion rate by reducing overall diffusion distance and this enhances the net reaction rate [28,29]. Hence, it is assumed that the lower crystallite size of treated CFA may improve its reaction rate [30] and it could be utilized for the synthesis of pharmaceutical compounds.

DSC analysis

The DSC was used to investigate the melting temperature and latent heat of fusion of the control and treated CFA. The DSC thermograms of control and treated CFA are presented in Figure 3. DSC of control CFA showed a sharp endothermic peak at 48.05°C which corresponded to melting temperature of the sample. However, the treated CFA showed a slight change in the melting temperature (47.56°C) as compared to the control sample. It was reported that the thermal energy required for completing the phase change from solid to liquid of a substance is known as the latent heat of fusion (ΔH). The latent heat of fusion of control CFA was 159.98 J/g; however after biofield treatment it was changed to 153.14 J/g. The result showed that latent heat of fusion of the treated CFA was changed by 4.27% with respect to the control. It is assumed that biofield treatment might altered the internal energy stored in the treated CFA which may lead to change in latent heat of fusion with respect to the control.

TGA-DTA analysis

TGA was conducted to investigate the thermal stability of control and treated CFA. The TGA thermogram of control CFA showed one-step thermal degradation (Figure 4). The thermal degradation commenced at around 140°C, and it was terminated at around 189°C in control sample. During this process, the sample lost 56.04% of its weight. However, the TGA thermogram of treated CFA showed thermal degradation at around 148 °C, and it was terminated at 185°C. During this event, the sample lost around 42.22% of its weight. Hence, the onset temperature was increased in treated CFA as compared to control. Additionally, the result showed a reduction in weight loss of the treated CFA with respect to the control.

The DTA thermogram of control and treated CFA are presented in Figure 4. DTA thermogram of control sample showed an endothermic peak at 170.89°C, which corresponded to thermal degradation temperature of the sample. Nevertheless, the treated sample exhibited an endothermic peak at 172.64°C that attributed to thermal degradation of the sample. The DTG thermogram of control and treated samples are presented in Figure 4. The temperature where maximum thermal decomposition (T_{max}) occurred is recorded from DTG and data are tabulated in Table 1. DTG of control sample showed T_{max} at 159.97°C; however it was increased to 163.34 °C in treated compound. The increase in T_{max} of biofield treated compound showed an increase in the thermal resistance with respect to the control. Overall, the increase in onset temperature, T_{max} and reduction in weight loss of treated sample showed the superior thermal stability as compared to the control. The increase in thermal stability of treated CFA was may be due to conformational changes and crosslinking caused by biofield treatment [31].

FT-IR spectroscopy

The FT-IR spectra of control and treated samples are shown in

Parameter	Control	Treated
Latent heat of fusion ΔH (J/g)	159.98	153.14
Melting temperature (°C)	48.05	47.56
T_{max} (°C)	159.97	163.34
Weight loss (%)	56.04	42.22

Table 1: Thermal analysis data of control and treated 3-chloro-4-fluoroaniline. T_{max}: Maximum thermal decomposition temperature.

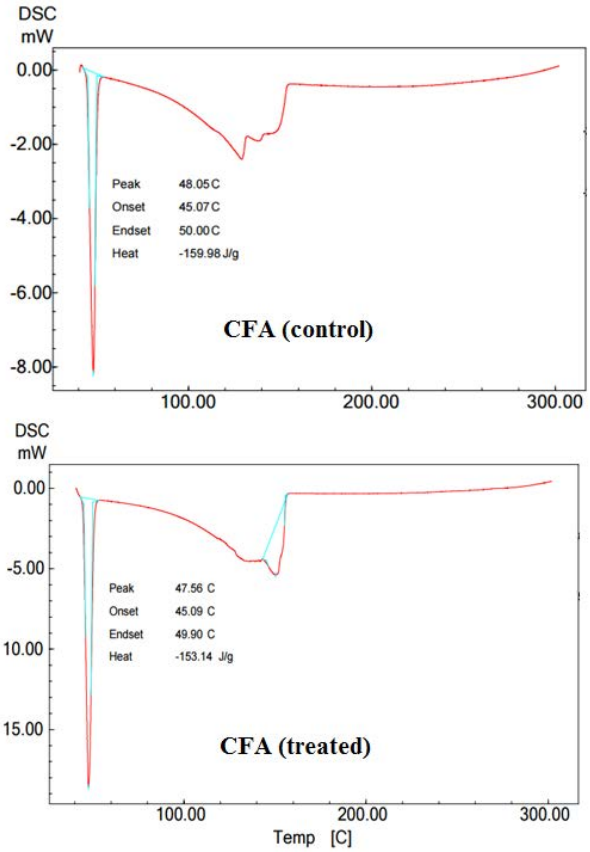

Figure 3: DSC thermogram of control and treated 3-chloro-4-fluoroaniline.

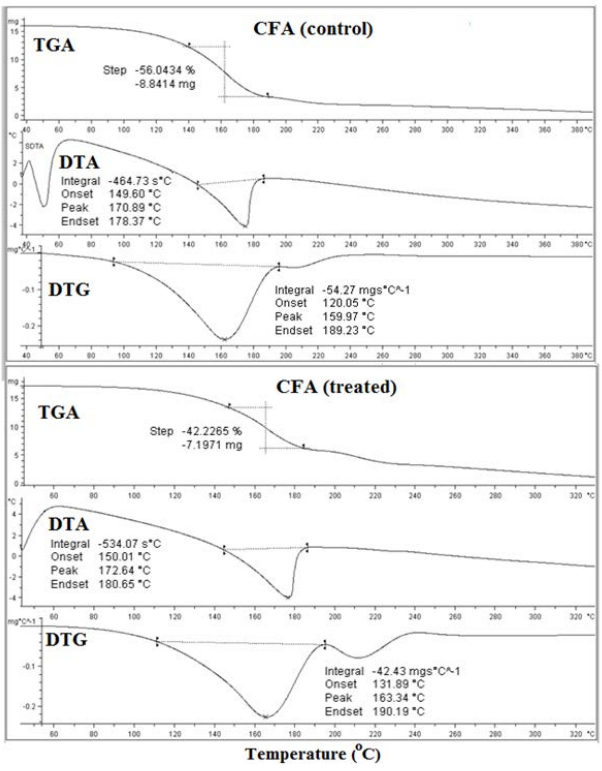

Figure 4: TGA thermogram of control and treated 3-chloro-4-fluoroaniline.

Figure 5. FT-IR spectrum of the control CFA showed characteristic peaks in the region of 3211-3439 cm^{-1} due to the N-H stretching vibration peaks. Vibration peak at 3049 cm^{-1} was due to the –CH aromatic stretching. Additionally, FT-IR peak at 1624 cm^{-1} was mainly due to the N-H bending vibration peak. The vibration peaks at 1500, 1599 cm^{-1} were corresponded to the C-C in ring stretching of aromatics. Absorption peaks at 1215 and 1259 cm^{-1} were due to the C-N stretching (aromatic) vibrations. The peak at 848 and 908 cm^{-1} were due to the –CH out of plane bending vibrations. Vibration peak at 769 cm^{-1} was attributed to chloro group attached to the phenyl ring [32]. The peak at 1045-1130 cm^{-1} were attributed to fluorine attached to the phenyl ring.

FT-IR spectrum of treated sample (T1) showed the N-H stretching vibration peaks in the region of 3211-3439 cm^{-1}. The –CH aromatic group stretching was observed at 3049 cm^{-1}. Vibrations peaks for the N-H bending and C-C in ring stretching were observed at 1620, 1599, and 1494 cm^{-1}. The C-N stretching vibration peaks were observed at 1215 and 1259 cm^{-1}. The C-H out of plane stretching vibrations were observed at 848 and 908 cm^{-1}. The C-Cl stretch was observed at 767 cm^{-1}. Additionally the absorption peaks in the region of 1045-1130 cm^{-1} were due to the fluorine group attached with phenyl ring.

The FT-IR spectrum of treated sample (T2) showed the N-H stretching vibration peaks in the region of 3215-3446 cm^{-1}. The –CH aromatic stretching was observed at 3049 cm^{-1}. Vibration peaks for the N-H bending and C-C in ring stretching were observed at 1637, 1602 and 1518 cm^{-1} respectively. The C-H out of plane bending vibrations were observed at 852 and 910 cm^{-1}. Vibration peak for a C-Cl stretch was observed at 775 cm^{-1}. The C-F stretching bond was observed in the range of 1057-1130 cm^{-1}. It is worthwhile to mention here that FT-IR spectrum of treated sample (T2) showed the emergence of new absorption peak at 3639 cm^{-1} that may be due to the intermolecular hydrogen bonding in the treated sample (T2). Moreover, the FT-IR spectrum of T2 sample showed an alteration in the region of 3439→3446 cm^{-1} (N-H stretch) and 1624-1637 cm^{-1} (N-H bending) which may be associated with an increase in hydrogen bonding after biofield treatment. Overall, the FT-IR result showed an increase in hydrogen bonding of treated CFA after biofield treatment as compared to the control.

UV-visible spectroscopy

UV spectra of control and treated CFA are shown in Figure 6. The UV spectrum of control CFA showed three absorption peaks *i.e.,* 205, 235 and 301 nm. The UV spectrum of CFA (T1) showed the occurrence of three absorption peaks *i.e.,* 210, 237 and 286 nm. However, the UV spectrum of CFA (T2) showed absorption peaks at 204, 235 and 301 nm. The results showed that as compared to the control alteration in absorption peaks was noticed in CFA (T1) sample. The absorption peak originally present at 205 nm in control, which was shifted to 210 nm in T1 sample. Additionally, the absorption peak present at 301 nm in control was shifted downward to 286 nm in T1 sample. According to Cinarli *et al.* the absorption peak appears in the region of 210-290 are mainly due to n→ π^* and π - π^* transition of the aromatic rings [33]. Hence it is assumed here that due to biofield treatment alterations occurred in electron *i.e.,* bonding (n→ π^* and $\pi \rightarrow \pi^*$ transition) from the ground state to excited state in the treated CFA as compared to the control.

Conclusion

In summary, the XRD analysis revealed a decrease in crystallite size by 22.08% in treated CFA as compared to the control. It is assumed

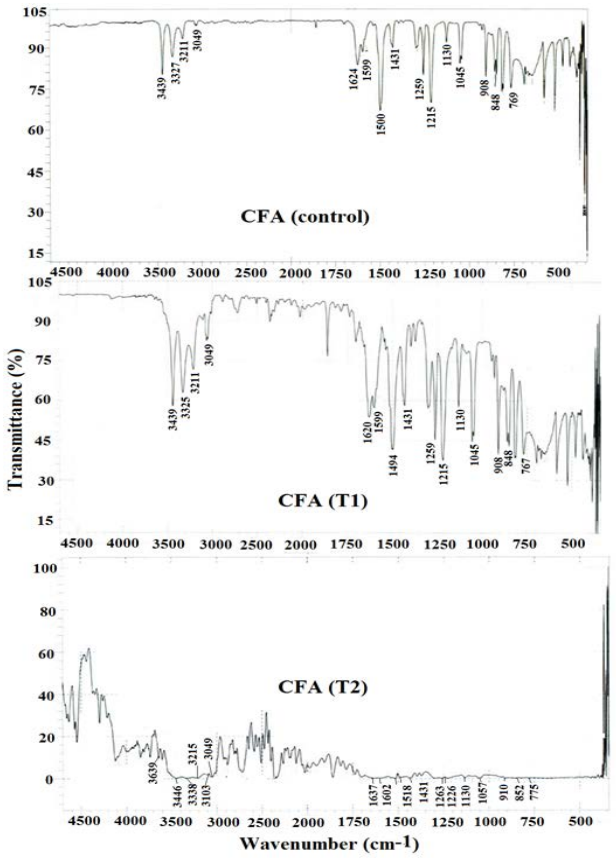

Figure 5: FTIR spectra of control and treated (T1 and T2) 3-chloro-4-fluoroaniline.

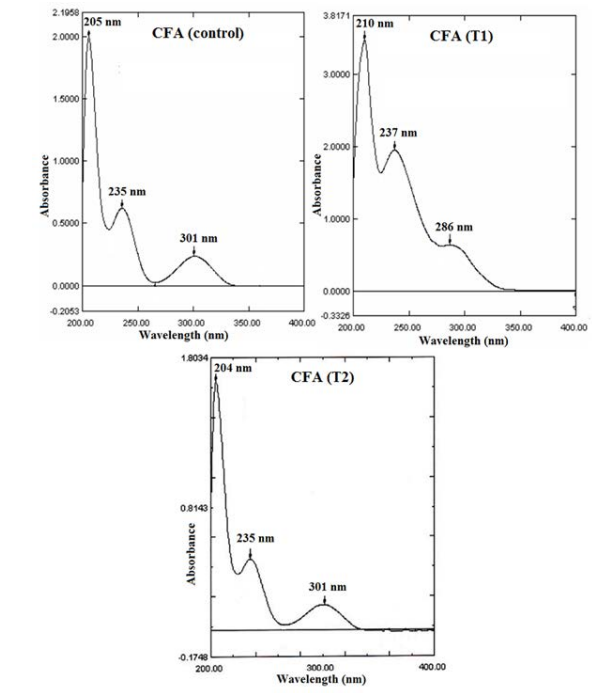

Figure 6: UV visible spectra of control and treated (T1 and T2) 3-chloro-4-fluoroaniline.

that occurrence of micro strain might cause a decrease in crystallite size in the treated CFA. However, the latent heat of fusion of treated sample was altered by 4.28% with respect to the control. The TGA analysis revealed an increase in T_{max}, and onset temperature as well as a reduction in the weight loss in treated sample as compared to the control. This indicated the increase in thermal stability of treated the CFA as compared to the control sample. The FT-IR spectroscopic analysis of treated CFA showed alterations in the N-H stretching and bending peaks as compared to the control. This may be due to biofield treatment that increased intermolecular hydrogen bonding in the sample as compared to the control. Additionally, UV-visible analysis showed alterations in absorption peaks of aromatic ring in the treated compound as compared to the control. The decrease in crystallite size, and increase in thermal stability of the treated sample showed that biofield energy treatment has significant impact on physical, thermal and spectral properties of CFA.

Acknowledgements

The authors would like to thank all the laboratory staff of MGV Pharmacy College, Nashik for their assistance during the various instrument characterizations. The authors would also like to thank Trivedi Science, Trivedi Master Wellness and Trivedi Testimonials for their support during the work.

References

1. Brycki B, Kowalczyk I, Werner J, Borowiak T, Wolska I, et al. (2006) Polyamines. I. Spectroscopic properties of N,N-bis-(phthalimidopropyl)-N-propylamine and supramolecular interactions in its crystals. J Mol Struct 791: 137-143.
2. Ranganathan A, Pedireddi VR, Rao CNR (1999) Hydrothermal synthesis of organic channel structures: 1:1 hydrogen-bonded adducts of melamine with cyanuric and trithiocyanuric acids. J Am Chem Soc 121: 1752-1753.
3. Boogaard PJ, Beulink GD, van Sittert NJ (1994) Biological monitoring of exposure to 3-chloro-4-fluoroaniline by determination of a urinary metabolite and a hemoglobin adduct. Environ Health Perspect 102 Suppl 6: 23-25.
4. Troy DB, Beringer P (2006) Remington: The Science and Practice of Pharmacy, Lippincott Williams and Wilkins, Baltimore, Maryland, USA.
5. Vardanyan R, Hruby V (2006) Synthesis of Essential Drugs. Elsevier, Amsterdam, Netherlands.
6. Blessy M, Patel RD, Prajapati PN, Agrawal YK (2014) Development of forced degradation and stability indicating studies of drugs- A review. J Pharm Anal 4: 159-165.
7. Trivedi MK, Patil S, Tallapragada RM (2013) Effect of biofield treatment on the physical and thermal characteristics of silicon, tin and lead powders. J Material Sci Eng 2: 125.
8. Trivedi MK, Patil S, Tallapragada RMR (2015) Effect of biofield treatment on the physical and thermal characteristics of aluminium powders. Ind Eng Manag 4: 151.
9. Trivedi MK, Patil S, Tallapragada RM (2013) Effect of biofield treatment on the physical and thermal characteristics of vanadium pentoxide powder. J Material Sci Eng S11: 001.
10. Trivedi MK, Nayak G, Patil S, Tallapragada RM, Jana S, et al. (2015) Bio-field treatment: An effective strategy to improve the quality of beef extract and meat infusion powder. J Nutr Food Sci 5: 389.
11. Trivedi MK, Patil S, Shettigar H, Bairwa K, Jana S (2015) Effect of biofield treatment on spectral properties of paracetamol and piroxicam. Chem Sci J 6: 98.
12. Barnes PM, Powell-Griner E, McFann K, Nahin RL (2004) Complementary and alternative medicine use among adults: United States, 2002. Adv Data: 1-19.
13. Aldridge D (1991) Spirituality, healing and medicine. Br J Gen Pract 41: 425-427.
14. Springhouse (1998) Nurses handbook of complementary and alternative therapies. (2nd edn), Lippincott Williams & Wilkins.
15. Rivera-Ruiz M, Cajavilca C, Varon J (2008) Einthoven's string galvanometer: the first electrocardiograph. Tex Heart Inst J 35: 174-178.

16. Movaffaghi Z, Farsi M (2009) Biofield therapies: biophysical basis and biological regulations? Complement Ther Clin Pract 15: 35-37.

17. Neuman MR (2000) Biopotential electrodes. The biomedical engg handbook: (2nd edn), Boca Raton: CRC Press LLC.

18. Shinde V, Sances F, Patil S, Spence A (2012) Impact of biofield treatment on growth and yield of lettuce and tomato. Aust J Basic Appl Sci 6: 100-105.

19. Sances F, Flora E, Patil S, Spence A, Shinde V, et al. (2013) Impact of biofield treatment on ginseng and organic blueberry yield. Agrivita J Agric Sci 35: 22-29.

20. Patil SA, Nayak GB, Barve SS, Tembe RP, Khan RR, et al. (2012) Impact of biofield treatment on growth and anatomical characteristics of Pogostemon cablin (Benth.). Biotechnology 11: 154-162.

21. Trivedi MK, Patil S, Shettigar H, Bairwa K, Jana S, et al. (2015) Phenotypic and biotypic characterization of Klebsiella oxytoca: An impact of biofield treatment. J Microb Biochem Technol 7: 203-206.

22. Trivedi MK, Patil S, Shettigar H, Gangwar M, Jana S, et al. (2015) An effect of biofield treatment on multidrug-resistant Burkholderia cepacia: A multihost pathogen. J Trop Dis 3: 167.

23. Pavia DL, Lampman GM, Kriz GS (2001) Introduction to spectroscopy. (3rd edn), Thomson Learning, Singapore.

24. Zhao Z, Du L, Tan Z (2014) Influence of electrodeposited crystallite size on interfacial adhesion strength of electroformed layers. Micro Nano Lett 9: 73-76.

25. Schicker S, Garcia DE, Gorlov I, Janssen R, Claussen N, et al. (1999) Wet milling of Fe/Al/Al2O3 and Fe2O3/Al/Al2O3 powder mixtures. J Am Ceram Soc 82: 2607-2612.

26. Muslimin M, Meor Yusoff MS (2009) The effect of high-energy milling on the crystallite size of alumina. JNRT 6: 95-102.

27. Mahmoud AE, Wasly HS, Doheim MA (2014) Studies of crystallite size and lattice strain in Al-Al2O3 powders produced by high-energy mechanical milling. J Eng Sci 42: 1430-1439.

28. Chaudhary AL, Sheppard DA, Paskevicius M, Webb CJ, Gray EM, et al. (2014) Mg2Si nanoparticle synthesis for high pressure hydrogenation. J Phys Chem C 118: 1240-1247.

29. Chaudhary AL, Sheppard DA, Paskevicius M, Saunders M, Buckley C (2014) Mechanochemical synthesis of amorphous silicon nanoparticles. R Soc Chem Adv 42: 21979-21983.

30. Chaudhary AL, Sheppard DA, Paskevicius M, Pistidda, C, Dornheim M, et al. (2015) Reaction kinetic behaviour with relation to crystallite/grain size dependency in the Mg–Si–H system. Acta Mater 95: 244-253.

31. Szabo L, Cik G, Lensy J (1996) Thermal stability increase of doped poly (3-hexadecylthiophene) by γ-radiation. Synt Met 78: 149-153.

32. http://orgchem.colorado.edu/Spectroscopy/specttutor/irchart.html.

33. Cinarli A, Gurbuz D, Tavman A, Birteksoz AS (2011) Synthesis, spectral characterizations and antimicrobial activity of some schiff bases of 4-chloro-2-aminophenol. Bull Chem Soc Ethiop 25: 407-417.